

Synthesis and Optical Properties of the Semiconductor Lead Sulfide Nanobelts

Xiao-hong Yang,^{1,2} Qing-Sheng Wu,^{1,*} Ya-Ping Ding,³ and Jin-ku Liu⁴

¹Department of Chemistry, Tongji University, Shanghai, 200092, P. R. China. *E-mail: qswu@mail.tongji.edu.cn

²Department of Chemistry, Chizhou Teacher College, Chizhou, Anhui, 247000, P. R. China

³Department of Chemistry, Shanghai University, Shanghai, 200436, P. R. China

⁴Department of Chemistry, East China University of Science and Technology, Shanghai 200237, P. R. China

Received August 29, 2005

The semiconductor PbS nanobelts (width 50-120 nm and length over 3 μm) were self-assembled in a simple reverse micelle solvent system containing the surfactant of polyoxyethylene (9) dodecyl ether (C_{12}E_9). The nanobelts synthesized were found to possess cube galena poly-crystal structure with high purity when analyzed by ED and X-ray diffraction. Significant "blue shift" from bulk material was observed on the PbS nanobelts using photoluminescence and UV-Vis spectroscopy. A mechanism involving the possible formation of nanobelts based on surfactant template was also proposed.

Key Words : Reverse micelles, Controlled synthesis, PbS, Nanobelt

Introduction

Due to its unique structure and superior optoelectronic properties, nanobelts have surpassed nanowires and nanotubes and attracted a lot of interest in nanomaterials research. The controlled synthesis of no-defective, oxide nanobelts under high temperature and the solid gas phase method was first described by Pan *et al.*¹ Since the one-dimensional nanobelts with wide band gap were expected to have vital applications in areas such as high-efficiency electricity transmission, a series of nanobelts have been fabricated,² most of which were oxides, such as ZnO, SnO₂, GaO₂, MoO₃, etc.³⁻⁵ There have also been a lot of interests in making nanobelts with non-oxide materials and potentially utilizing them in areas such as electronics, biology, pigment and pharmaceuticals. The most commonly study of non-oxide semiconductors focus on sulfides, such as CdS, ZnS, Bi₂S₃, Ti₂S, etc.⁶⁻¹⁰ However, synthesis of nanobelts has proven to be difficult because reactions are often performed at very high temperature and require the addition of catalysts. Therefore, it is important to explore the simple and mild methods to achieve the controlled synthesis of nanobelts, preferably under room temperature.

As typical narrow band gap semiconductors, PbS nanomaterials possess special optoelectronic properties, which have vital applications in optical information storage, optical communication apparatus, radioactivity detector, etc.¹¹⁻¹³ A number of PbS nanomaterials with different morphologies and structures such as nanoparticles,¹⁴ nanorods,¹⁵ nanowires,¹⁶ nanoflakes,^{17,18} and nanocubes¹⁹ have been synthesized. However, so far there is no report so far on the synthesis of nanobelts by employing using the reverse micelles under a mild chemical reaction condition and at room temperature.

The reverse micelle soft-template method represents a simple and unique way to make nanomaterials with desired nano-sizes and two- or three-dimensional tropism. Compar-

ed with nanomaterials obtained from physical-chemical methods, the products prepared in reverse micelles are widely considered to show superior structures and physical properties.²⁰ Herein, this paper describes a successfully self-controlled synthesis of PbS nanobelts in a reverse micelle system by employing the surfactant of C_{12}E_9 as the soft template. The optical properties of PbS nanobelts are investigated and the potential mechanism of reaction is also proposed.

Experimental Section

Reagents and Equipment. C_{12}E_9 [polyoxyethylene (9) dodecyl ether], cyclohexane, absolute ethanol, *n*-pentanol, $\text{Na}_2\text{S}\cdot 9\text{H}_2\text{O}$ and $\text{Pb}(\text{CH}_3\text{COO})_2\cdot 3\text{H}_2\text{O}$ were purchased from Shanghai Chemical Reagent Factory, China. All the reagents are of analytical grade.

The morphologies of the products were observed through transmission electron microscopy (TEM). The crystal phase and structure of the products were determined by X-ray powder diffraction (XRD) using Hitachi-800 diffractometer with graphite monochromatized $\text{Cu-K}\alpha$ radiation ($\lambda = 0.15418$ nm, 50 kV, 100 mA). Optical properties of products were studied by Agilent 8453 UV-Visible spectrophotometer, Perking Elmer LS-55 fluorescent spectroscopy.

Preparation of the PbS Nanobelts. The reverse micelle system was prepared by adding into a 250 mL volumetric glass in sequence of 28 mL cyclohexane, 3 mL C_{12}E_9 , 1 mL of 0.1 mol/L aqueous $\text{Pb}(\text{CH}_3\text{COO})_2\cdot 3\text{H}_2\text{O}$ and 1 mL *n*-pentanol. The same experiment was also performed in parallel by adding into another 250 mL volumetric glass in sequence of 28 mL cyclohexane, 3 mL C_{12}E_9 and 1 mL of 1.0 mol/L aqueous $\text{Na}_2\text{S}\cdot 9\text{H}_2\text{O}$. Both solutions were mixed vigorously at approximately 3000 rpm for 15 minutes, and kept at room temperature for another five minutes. After that an equal volume of two microemulsions, one containing S^{2-} and the other containing Pb^{2+} , was mixed together followed

by gentle shaking for another 5 to 10 minutes. The final solution was kept at room temperature for 12 hours to result in the formation of nanobelts.

A volume of 3 mL acetone was then added to the solution to break up the micelles. Finally, the supernatant was removed from the solution described above, the bottom solution was centrifuged at 2000 rpm for 10 minutes, washed sequentially with acetone, ethanol and water 2-3 times each. The final product should be black precipitate insoluble in water and ethanol.

The morphology of the final product was observed using TEM. One to two drops of the microemulsion solutions containing the PbS products were transferred onto a copper grid that was placed on filter paper followed by air-drying. The structure of the final product was studied using X-ray diffraction, while the optical properties of the product was determined by photoluminescence (PL) and UV-Vis spectrophotometers.

Results and Discussion

Morphologies and Structures. The TEM micrograph and electron diffraction of the PbS nanoproducts formed are shown in Figure 1. The products have belt shape (Figure 1a). The single layer nanobelts were very thin and nearly transparent. There were also some other nanobelts shown in Figure 1a, which were likely made of a few overlapping layers. The width of the nanobelt was found to be between 50 and 120 nm and the length over 3 μm . The exact thickness of the nanobelts can't be easily measured. However, it was concluded that nanobelts should be approximately 3 nm thick based on: (1) As pointed in the arrow in Figure 1a, the particles were still visible even when they were underneath the nanobelt. This has clearly demonstrated the transparent nature of the nanobelt and subsequently shown the thickness of the nanobelt was under 5 nm. (2) As shown in Figure 1b, the nanobelts could be penetrated by 100 kv electron beam. This has proven the nanobelt was less than 20 nm in thickness. (3) "Blue Shift" was observed on the UV-Vis absorption spectrum of the PbS nanobelts (in Figure 3). The thickness of the nanobelts was thus determined to be around

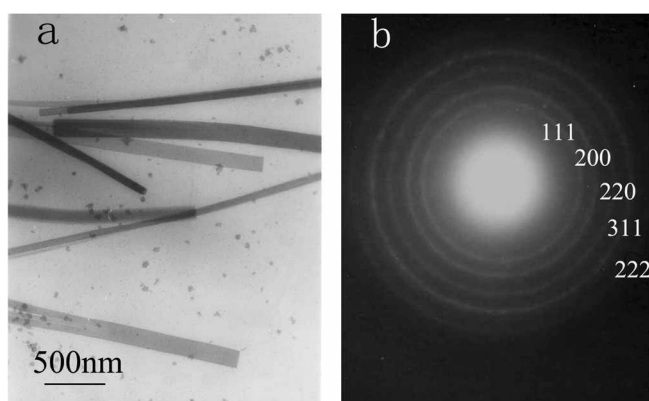


Figure 1. The TEM micrograph (a) and ED image (b) of PbS nanobelts.

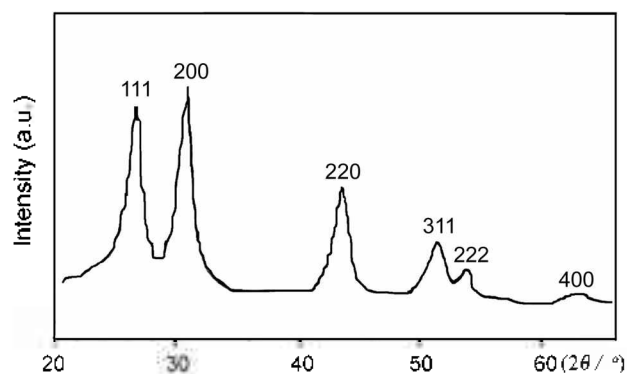


Figure 2. The XRD pattern of the PbS nanobelts.

3 nm based on literature report.²¹ (4) As shown in Figure 5, the gap between different layers of micelles was normally 1-4 nm.²² This has in turn limited the nanobelt thickness to 1-4 nm.

The corresponding electron diffraction pattern has shown the presence of clear diffraction circles, indicative of polycrystal structure. No impurity peaks were observed from the XRD spectral of the nanobelts (Figure 2). All the peaks found in Figure 2 matched with the ones listed in *JC-PDS* file (No: 5-592) for the cube galena structure. The lattice constant was then calculated to be 5.9378 Å, close to the *JC-PDS* file. Therefore, it was concluded that very pure PbS nanobelts were synthesized in this experiment and the nanobelts possessed cube galena polycrystal structure.

Experimental Conditions. Experimental conditions have been optimized in order to produce the PbS nanomaterial with the desired dimension, morphologies and structures. (1) It was found that the concentrations of reactant have influence on morphologies and structures of the products. When the concentration of Pb^{2+} and S^{2-} were 0.1 mol/L respectively, the products were nanorods (shown in Figure 3a), not nanobelts. When the concentration of Pb^{2+} and S^{2-} were 1.0 mol/L respectively, the products were large particles (shown in Figure 3b), not nanorods or nanobelts. The excess amount of S^{2-} was important. It not only

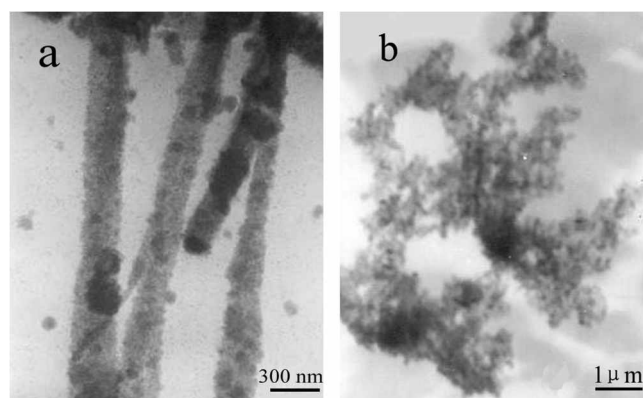


Figure 3. The TEM micrograph of PbS products (When the concentration of Pb^{2+} and S^{2-} were a 0.1 mol/L; b When the concentration of Pb^{2+} and S^{2-} were 1.0 mol/L, respectively).

improved the morphologies of the final nanobelts, but also ensured the complete depletion of Pb^{2+} to avoid the environmental pollutions from heavy metal waste. In this paper the concentration ratio of S^{2-} to Pb^{2+} was 10. A concentration of 0.1 mol/L for $Pb(CH_3COO)_2 \cdot 3H_2O$ and that of 1.0 mol/L of $Na_2S \cdot 9H_2O$ were used in the experiments described in this paper. (2) Molar ratio of the water to the surfactant was ten on the experiments described in this paper. Theoretically, surfactant to *n*-pentanol volume ratio (δ) had no effect on the reverse micelle system containing $C_{12}E_9$. However, a δ value of three was selected here for the solution containing $Pb(CH_3COO)_2 \cdot 3H_2O$ to improve emulsion, and no *n*-pentanol was added to the solution containing $Na_2S \cdot 9H_2O$ as determined to be unnecessary.

Optical Properties. As shown in the UV-Vis absorption spectra in Figure 3, a strong absorption peak was observed at the wavelength about 347 nm for the PbS nanobelts. Due to its semiconductor nature, the PbS nanobelts have demonstrated excellent photoluminescence (PL) properties. When excited at 390 nm, nanobelts have shown a significant "blue shift" with the new emission wavelength peaking at 423 nm. Unlike the bulk materials,²³ the PbS nanobelts have shown

narrow gap band (0.41 eV) and large Bohr exciton radius. This has resulted in strong quantum confinement effect, unique three stage non-linear optical properties and properties of optical band restriction found on the PbS nanobelts.

Formation Mechanism of Nanobelts. The process of nanobelts synthesis is relatively complexed. A microemulsion template based mechanism is proposed below to explain the formation process of nanobelts in the reverse micelle system containing $C_{12}E_9$. It has been reported previously that different surfactants or even the same surfactant at different concentrations may have provided different microemulsion soft templates that resulted in the formation of nanomaterials with different morphologies and structures, such as spheres, rods, layers, etc.²⁴ The surfactant of $C_{12}E_9$ is a relatively simple and symmetric molecule (Figure 4). The hydrophilic oxy-ethylene chain tended to arrange along the surface and formed the colloids of layer shape. This has subsequently provided the microemulsion template leading to the directional aggregation of PbS colloid nanoparticles.

PbS nucleuses were formed as soon as the reverse micelles containing S^{2-} and Pd^{2+} were mixed. The nucleuses would penetrate each other and amalgamate; the PbS nanoparticles were then produced. Guided by the microemulsion soft template, the nanoparticles aligned along the plane surface. The gap between different layers would shrink due to the interaction between the hydrophilic groups of $C_{12}E_9$ molecules. Finally, a very thin layer of nanobelt was obtained after removing template (Figure 5).

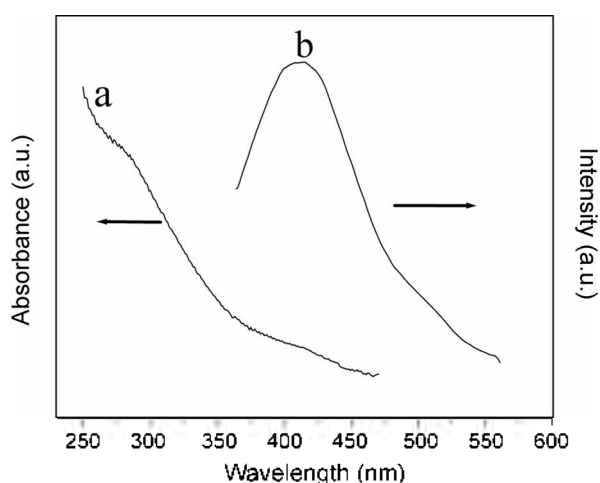


Figure 4. The UV-Vis spectra (a) and PL spectra (b) of the PbS nanobelts.

Conclusion

The synthesis of the non-oxide nanobelts is traditionally considered to be technically very challenging. Although the reverse micelle systems have been employed to prepare nanomaterials with various morphologies and structures, the synthesis of the nanobelts using the reverse micelles isn't still reported. As described in this paper, PbS nanobelts were formed at the room temperature using the reverse micelles technique that included the surfactant of $C_{12}E_9$. The method used is simple, easy, mild and controllable.

Significant "blue shift" was observed on the PbS nano-

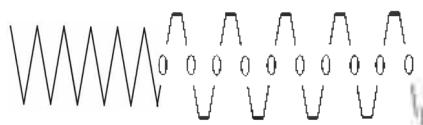
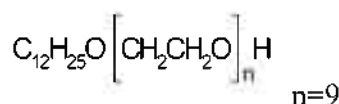


Figure 5. Chemical structure of the $C_{12}E_9$.

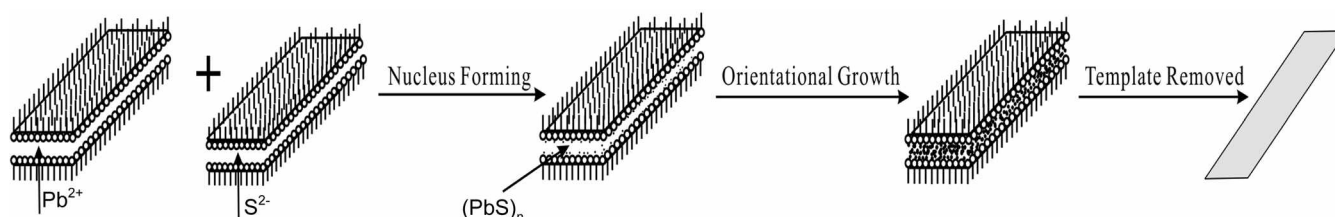


Figure 6. The proposed formation mechanism of PbS nanobelts.

belts when analyzed by photoluminescence and UV-Vis spectroscopy. Nanobelts have thus demonstrated even more superior optoelectronic properties than nanowires and nanotubes. Therefore, they are expected to show vital applications in many important areas. A microemulsion templates based assembling process was proposed as the mechanism of synthesis. However, a lot more studies are still needed in order to fully understand the mechanism for the formation of nanobelts in the reverse micelle systems containing the surfactant of C₁₂E₉.

Acknowledgements. The authors are grateful to the financial support of the National Natural Science Foundation of China (Grant No: 20471042 and 20571051); Nano-Foundation of Shanghai in China (Grant No: 0452nm075) and the Doctoral Program Foundation of the Ministry of Education (Grant No: 20040247045).

References

1. Pan, W. Z.; Dai, Z. R.; Wang, Z. L. *Science* **2001**, *291*, 1947.
2. Zhang, M.; Wang, Z. H.; Xi, G. C.; Ma, D.; Zhang, R.; Qian, Y. J. *Crystal Growth* **2004**, *268*, 215.
3. Dai, Z. R.; Pan, Z. W.; Wang, Z. L. *Adv. Func. Mater.* **2003**, *13*, 9.
4. Chen, Y. J.; Li, Q. H.; Liang, Y. X.; Wang, T. H.; Zhao, Q.; Yu, D. *P. App. Phys. Lett.* **2004**, *85*, 5682.
5. Zhang, J.; Jiang, F.; Zhang, L. *J. Phys. Chem. B* **2004**, *108*, 7002.
6. Gao, T.; Wang, T. *J. Phys. Chem. B* **2004**, *108*, 5.
7. Liang, C. H.; Shimizu, Y.; Sasaki, T.; Umehara, H.; Koshizaki, N. *J. Phys. Chem. B* **2004**, *108*, 9728.
8. Li, Y. J.; You, L. P.; Duan, R.; Shi, P. B.; Du, H. L.; Qiao, Y. P.; Qin, G. G. *Nanotechnology* **2004**, *15*, 581.
9. Hu, P.; Liu, Y.; Fu, L.; Cao, L.; Zhu, D. *J. Phys. Chem. B* **2004**, *108*, 936.
10. Ma, B. C.; Moore, D.; Li, J.; Wang, Z. L. *Adv. Mater.* **2003**, *15*, 228.
11. Zhou, Y.; Itoh, H.; Uemura, T.; Naka, K.; Chujo, Y. *Langmuir* **2002**, *18*, 5287.
12. Winiarz, J. G.; Zhang, L.; Park, J.; Prasad, P. N. *J. Phys. Chem. B* **2002**, *106*, 967.
13. Leontidis, E.; Orphanou, M.; Kyprianidou-Leodidou, T.; Krumeich, F.; Caseri, W. *Nano Lett.* **2003**, *3*, 569.
14. Zeng, Z. H.; Wang, S. H.; Yang, S. H. *Chem. Mater.* **1999**, *11*, 3365.
15. Wang, S.; Yang, S. *Langmuir* **2000**, *16*, 389.
16. Ge, J. P.; Wang, A.; Zhang, H. X.; Wang, X.; Peng, Q.; Li, Y. D. *Chem. Eur. J.* **2005**, *11*, 1889.
17. Yu, D.; Wang, D.; Zhang, S.; Liu, X.; Qian, Y. *J. Crystal Growth* **2003**, *249*, 195.
18. Zhou, S. M.; Zhang, X. H.; Meng, X. M.; Fan, X.; Lee, S. T.; Wu, S. K. *J. Solid State Chem.* **2005**, *178*, 399.
19. Kuang, D.; Xu, A.; Fang, Y.; Liu, H.; Frommen, C.; Fenske, D. *Adv. Mater.* **2003**, *15*, 1747.
20. Zhang, N. W.; Wu, Q. S.; Ding, Y. P.; Li, Y. D. *Chem. Lett.* **2000**, *6*, 638.
21. Machol, J. L.; Wise, F. W.; Patel, R. C.; Tanner, D. B. *Phys. Rev. B* **1993**, *48*, 2819.
22. Zhang, W. R.; Zhang, S. Y.; Zhang, Y. C. *Surfactant, Anhe.*; College Publishing Company: Hefei, 1997; p 106.
23. Daven, R. *Infrared, Phys.* **1969**, *9*, 141.
24. Liu, J.; Kim, A. Y.; Wang, L. Q.; Palmer, B. J.; Chen, Y. L.; Bruinsma, P.; Bunker, B. C.; Exarhos, G. J.; Graff, G. L.; Rieke, P. C.; Fryxell, C. E.; Virden, J. W.; Tarasevich, B. J.; Chick, L. A. *Adv. Colloid Interface Sci.* **1996**, *69*, 131.